





Copyright@Author(s) - Available online at dirjournal.org. Content of this journal is licensed under a Creative Commons Attribution-NonCommercial 4.0 International License. ORIGINAL ARTICLE

# A diagnostic model based on magnetic resonance imaging for Menière's disease: a multicentre study

- Xinyi Chen<sup>1\*</sup>
- Yunchong Han<sup>3</sup>
- Kai Wei<sup>1</sup>
- Shufang Cheng<sup>4</sup>
- Yongjun Ye<sup>4</sup>
- Jie Feng<sup>4</sup>
- Xinchen Huang<sup>1</sup>
- Jingjing Xu<sup>1</sup>

<sup>1</sup>Zhejiang University School of Medicine, The Second Affiliated Hospital, Department of Radiology, Hangzhou, China

<sup>2</sup>Chinese Academy of Medical Sciences and Peking Union Medical College, National Cancer Center, Cancer Hospital, National Clinical Research Center for Cancer, Department of Radiology, Beijing, China

<sup>3</sup>The Second Affiliated Hospital of Jiaxing University, Department of Radiology, Jiaxing, China

<sup>4</sup>The Fifth Affiliated Hospital of Wenzhou Medical University, Zhejiang Key Laboratory of Imaging and Interventional Medicine, Lishui, China

#### **PURPOSE**

To evaluate the diagnostic performance of delayed post-gadolinium enhancement magnetic resonance imaging (DEMRI) in diagnosing Menière's disease (MD) and to establish an effective MRI-based diagnostic model.

#### **METHODS**

This retrospective multicenter study assessed DEMRI descriptors in patients presenting with Ménièriform symptoms who were examined consecutively between May 2022 and May 2024. A total of 162 ears (95 with MD, 67 controls) were included. Each ear was randomly assigned to either a training set (n = 98) or a validation set (n = 64). In the training cohort, diagnostic models for MD were developed using logistic regression. The area under the curve (AUC) was used to evaluate the diagnostic performance of the different models. The Delong test was applied to compare AUC estimates between models.

#### **RESULTS**

The proposed DEMRI diagnostic model demonstrated strong diagnostic performance in both the training cohort (AUC: 0.907) and the validation cohort (AUC: 0.887), outperforming the clinical diagnostic model (P = 0.01231; 95% confidence interval: 0.033-0.269) in the validation cohort. The AUC of the DEMRI model was also higher than that of the combined DEMRI-clinical model (AUC: 0.796), although the difference was not statistically significant (P = 0.054). In the training set, the sensitivity and specificity of the DEMRI model were 78.9% and 88.5%, respectively.

### CONCLUSION

A diagnostic model based on DEMRI features for MD is more effective than one based solely on clinical variables. DEMRI should, therefore, be recommended when MD is suspected, given its significant diagnostic potential.

# **CLINICAL SIGNIFICANCE**

This model may improve the accuracy and timeliness of MD diagnosis, as it is less influenced by the attending physician's level of inquiry or the patient's self-reporting ability. It may also contribute to more effective disease management in patients with MD.

## **KEYWORDS**

Post-gadolinium enhancement magnetic resonance imaging, Menière's disease, endolymphatic hydrops, diagnosis, model

#### \*Joint first authors

Corresponding author: Jingjing Xu

E-mail: jingjingxu@zju.edu.cn

Received 19 February 2025; revision requested 17 March 2025; accepted 13 April 2025.



Epub: 29.05.2025

Publication date: 08.07.2025

DOI: 10.4274/dir.2025.253293

enière's disease (MD) is a multifactorial condition in which the combined effect of genetic and environmental factors may determine its onset.¹ The main clinical symptoms include idiopathic fluctuating sensorineural hearing loss (SNHL), spontaneous vertigo, aural fullness, and tinnitus. Prosper Ménière first described the disease in 1861, proposing that the pathological site was in the labyrinth rather than the brain.²³ However, diagnosis has been challenging, especially when the initial symptoms are subtle, resulting in limited studies on the epidemiology of MD. The American Academy of Otolaryngology–Head

You may cite this article as: Chen X, Zhao Y, Han Y, et al. A diagnostic model based on magnetic resonance imaging for Menière's disease: a multicentre study. Diagn Interv Radiol. 2025;31(4):347-358. and Neck Surgery developed guidelines for the diagnosis and therapeutic evaluation of MD in 1972, which were revised in 1985 and 1995.<sup>4</sup> In 2015, the Barany Society updated and established consensus diagnostic criteria for MD, partly to distinguish migraine-related vertigo from MD.<sup>5,6</sup> However, these updated criteria still relied on patient self-reports rather than objective medical tests. In addition, an insufficient understanding of MD in some clinical departments has led to delayed diagnosis and treatment.

In 1937, British and Japanese researchers discovered endolymphatic hydrops (EH) in the human temporal bone and provided a pathological description of Menière's syndrome.<sup>7,8</sup> In 2007, Nakashima et al.<sup>9</sup> successfully demonstrated EH in a patient with MD using delayed inner ear imaging with a three-dimensional fluid-attenuated inversion recovery (3D-FLAIR) sequence after intratympanic gadolinium injection. Since then, a series of magnetic resonance imaging (MRI) studies on EH have emerged.8,10-14 3D-FLAIR and three-dimensional inversion recovery with real reconstruction (3D-real IR) are the most commonly used imaging sequences for EH.11 With these newer imaging techniques, EH can be visualized in vivo and used to support diagnosis. In addition to EH, several other signs<sup>1-20</sup> can also be observed on MRI. As a non-invasive tool, the diagnostic performance of delayed post-gadolinium enhancement MRI (DEMRI) remains to be fully clarified.

The aim of this study is to establish an intuitive and objective diagnostic model for MD, providing an effective diagnostic pathway for patients, improving the efficiency and accuracy of diagnosis, and offering a reference for clinical treatment planning.

# **Main points**

- Delayed post-gadolinium enhancement magnetic resonance imaging (DEMRI) of the inner ear enables visualization of endolymphatic hydrops and perilymphatic spaces in patients with Menière's disease (MD), which is critical for diagnosis.
- In the DEMRI-based diagnostic model, the most substantial features were "Cochlea\_ EH\_Grad," "Cochlea\_Apex\_EH\_Score," "VA," and "Vestibule\_EH."
- The diagnostic performance of DEMRI for MD is superior to that of clinical information alone.

# **Methods**

### **Patients**

This multicenter retrospective study followed the principles outlined in the Declaration of Helsinki, including all amendments and revisions. The research was approved by the Medical Ethics Committee of the Second Affiliated Hospital of Zhejiang University School of Medicine IRB-2024-0048 (date: 13.05.2024). Informed written consent was obtained from all participants after an explanation of the nature of the study, as approved by the same ethics committee.

This retrospective study included data from consecutive patients who first visited the otology departments of three medical centers with Menièriform symptoms such as vertigo, hearing loss, tinnitus, and aural fullness and who underwent DEMRI of the inner ear labyrinth between May 2022 and May 2024. A total of 136 patients (272 ears) were retrospectively analyzed. Ultimately, 85 patients (162 ears: 95 MD ears, 67 control ears; mean age: 55.2 ± 13.6 years) were enrolled in the study based on the exclusion criteria (Figure 1). Each ear was treated as a single unit and randomly assigned to either a training set (n = 98 ears) or a validation set (n = 64ears) in a 6:4 ratio (Figure 1).

Baseline clinical data, including sex, age, affected side, inner ear symptoms (vertigo, hearing loss, tinnitus, aural fullness), and pure tone audiometry (PTA), were extracted from the medical record management

system. Given variations in clinical inquiry, symptoms such as vertigo, hearing loss, tinnitus, and aural fullness were recorded as either "yes" or "no," excluding frequency and duration as specified in the diagnostic criteria for MD. Based on the average hearing threshold from PTA at 0.5 kHz, 1 kHz, and 2 kHz, hearing loss was classified into four stages: stage I = average hearing threshold ≤ 25 dB HL; stage II ≥ 25–40 dB HL; stage III ≥ 40–70 dB HL; and stage IV = average hearing threshold > 70 dB HL.

# Magnetic resonance imaging examinations

Patients underwent DEMRI using 3T scanners at the participating centers (Center A: uMR 790, UIH, Shanghai, China; Ceners B and C: Ingenia CX, Philips Healthcare, Netherlands) with a standard 32-channel head and neck coil. Prior to gadolinium administration, a 3D-T2-sampling perfection with application-optimized contrasts using different flip angle evolutions (3D-T2-SPACE) sequence was performed with the following parameters: repetition time (TR): 1300 ms; echo time (TE): 196.68 ms; slice thickness: 0.5 mm; matrix size:  $380 \times 100$ ; field of view (FOV): 220 × 180 mm; acceleration factor: 2 (2D); scan time: 1 min 47 s. This scan was used to exclude patients with organic brain syndromes, inner ear malformations, or acoustic neuro-

A 3D-FLAIR sequence was performed 4 hours after administration of a double dose of intravenous gadobutrol (7.5 mL/vial, 1.0 mmol/mL; Bayer AG) to ensure maximum

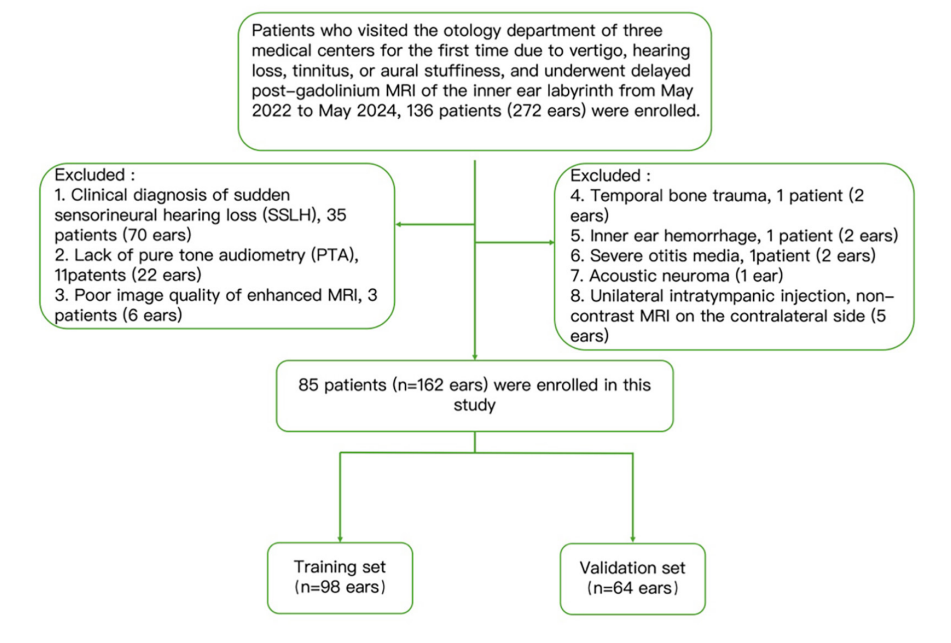


Figure 1. Flowchart of the patient recruitment pathway. MRI, magnetic resonance imaging.

perilymphatic enhancement (PLE). Imaging parameters were: FOV:  $220 \times 190$  mm; section thickness: 0.7 mm; TR: 6500 ms; TE: 426 ms; number of excitations = 1; inversion time = 1935 ms; flip angle =  $54^\circ$ ; matrix:  $256 \times 100$ ; bandwidth: 500 Hz/pixel; turbo factor: 5 (acs); voxel size:  $0.86 \times 0.86 \times 1$  mm; scan time: 2 min 56 s. Previous studies<sup>21,22</sup> have shown that gadobutrol offers advantages over other macrocyclic gadolinium contrast agents in MRI for diagnosing MD due to its higher concentration and greater relaxivity.

# Extraction of qualitative and quantitative magnetic resonance imaging features

The MR images were qualitatively analyzed by three experienced radiologists (with 15, 15, and 20 years of experience in head and neck imaging diagnosis, respectively), all blinded to the clinical findings and symptoms.

The degree of EH was indicated by a widening of the negative signal gap within the labyrinth. In this study, the cochlea and vestibule were dichotomized as EH-positive or EH-negative based on the presence or absence of hydrops. Cochlear and vestibular EH grades were evaluated using the visual four-grade method proposed by Gürkov and Bernaerts.<sup>23,24</sup>

# Cochlea

- Normal (grade 0): The scala media (SM) appeared as a vaguely visible dark area with a relatively straight border separating it from the scala vestibuli and scala tympani (Figure 2a).
- Mild hydrops (grade 1): The SM exhibited a distinct hypointense area surrounded by a clear and continuous hyperintense perilymphatic ring (Figure 2b).
- Moderate hydrops (grade 2): The hyperintense perilymphatic ring was substantially interrupted (Figure 2c).
- Severe hydrops (grade 3): The surrounding hyperintense perilymphatic area became a clear, straight line (Figure 2d).

# Vestibule

- Normal (grade 0): The saccule and utricle were separated, and their combined area occupied less than half of the vestibular space (Figure 3a).
- Mild hydrops (grade 1): The saccule was equal to or larger than the utricle, and the two could still be distinguished (Figure 3b).

- Moderate hydrops (grade 2): The saccule and utricle were fused, but peripheral perilymph remained visible (Figure 3c).
- Severe hydrops (grade 3): No PLE was observed in the vestibule (Figure 3d).

In addition, a new weighted visual scoring system based on the Inner Ear Structural Assignment Method<sup>25,26</sup> was employed (Table 1). The signal intensity ratio of PLE to the ipsilateral middle cerebellar peduncle was measured. The semicircular canals and vestibular aqueduct (VA) were graded as 0, 1, or 2, depending on whether they were continuously developed. In total, six clinical variables and 17 MRI features were included in the analysis (Supplementary Table 1).

# Statistical analysis

To analyze all data, IBM SPSS (version 27.0) and R software (version 4.2.1) were used. Continuous variables were presented as mean  $\pm$  standard deviation or median with interquartile range. Measurement data conforming to a normal distribution were compared using the independent sample t-test. The Mann–Whitney U test was used to compare measurement data that did not conform to a normal distribution. Categorical data were compared using the  $\chi^2$  test or Fisher's exact test. Kendall's W test was used to assess inter-observer agreement.

Multivariable logistic regression analysis was applied to select MD-related features. Variables with P < 0.05 were included in the

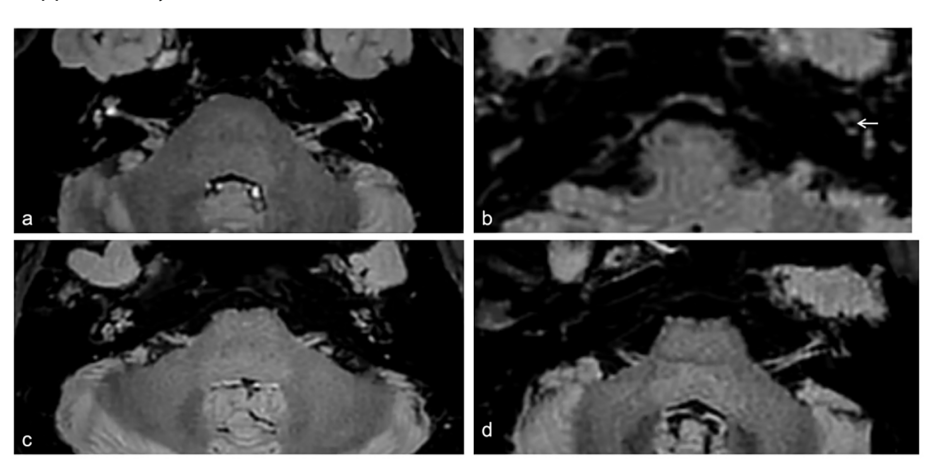
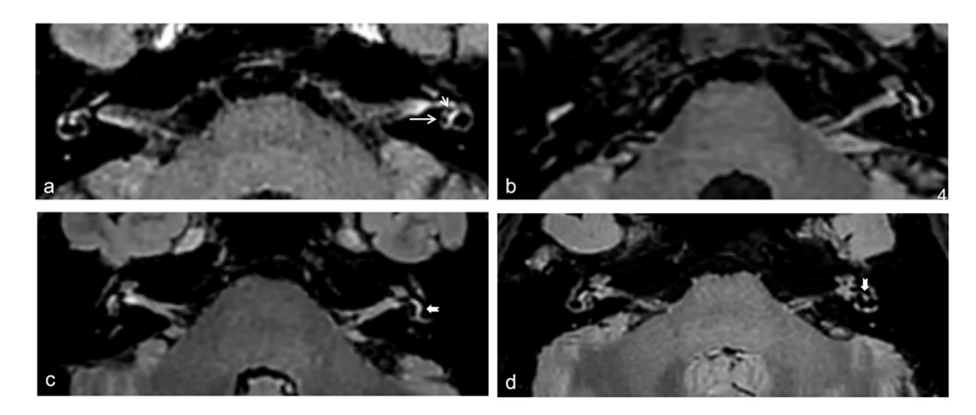


Figure 2. Grading of cochlear hydrops on axial 3D-FLAIR delayed-enhancement images. Grade 0 (normal): The scala media (SM) appears as a faint dark area (arrow) with a relatively straight border between the scala vestibuli and scala tympani (a). Grade 1 (mild hydrops): The SM shows a distinct nodular low signal area (white arrow), surrounded by a clear, continuous high-signal perilymphatic ring (b). Grade 2 (moderate hydrops): The high-signal perilymphatic ring is substantially interrupted (left arrow) (c). Grade 3 (severe hydrops): The surrounding high-signal perilymphatic area appears as a thin, straight line (left arrow) (d). 3D-FLAIR, three-dimensional fluid-attenuated inversion recovery.



**Figure 3.** Grading of vestibular hydrops on axial 3D-FLAIR delayed-enhancement images. Grade 0 (normal): The saccule (short arrow) and utricle (long arrow) remain separated; the combined area is less than half of the vestibule (a). Grade 1 (mild hydrops): The saccule is equal to or larger than the utricle (arrow), but the two structures remain distinct (b). Grade 2 (moderate hydrops): The saccule and utricle are fused; peripheral perilymph remains visible (swallow-tail arrow, (c). Grade 3 (severe hydrops): Complete loss of perilymphatic enhancement in the vestibule (swallow-tail arrow, (d). 3D-FLAIR, three-dimensional fluid-attenuated inversion recovery.

multivariate logistic regression model using the backward stepwise method to develop three models for MD diagnosis in the training cohort: DEMRI signature, clinical variables, and combined DEMRI-clinical parameters. The validation set was used to validate these models. The area under the curve (AUC) of the receiver operating characteristic (ROC) curve was used to evaluate the diagnostic performance of the different models. The DeLong test was used to compare the AUC values between the models. A two-tailed *P* value less than 0.05 was considered statistically significant. The equation of the multivariate logistic regression model was as follows:

$$P(y=1|x_1,x_2,...,x_m) = rac{1}{1+e^{-(eta_0+eta_1x_1+eta_2x_2+...+eta_mx_m)}}$$

# **Results**

PE/MCPE

#### **Patient characteristics**

A total of 85 patients (162 ears; mean age:  $53.2 \pm 13.6$  years; age range: 17-86 years) were included. The detailed clinical and DEMRI characteristics of all ears in the

MD group (n = 95) and the control group (n = 67) are presented in Supplementary Table 1. Except for sex, body mass index, and VA visualization degree, all other observed indicators differed significantly between the MD and control groups (P < 0.05). The detailed characteristics of ears in the training set (n = 98) and validation set (n = 64) are shown in Supplementary Table 2.

# Diagnostic model development and valida-

In the training set, 17 DEMRI-independent descriptors were analyzed using multivariate logistic regression with backward stepwise selection. Four descriptors with *P* < 0.05 (Table 2) were selected to construct the DEMRI diagnostic model, which showed strong diagnostic performance for MD, with an AUC of 0.907 [95% confidence interval (CI): 0.848–0.966] in the training cohort and 0.887 (95% CI: 0.802–0.971) in the validation cohort (Figures 4a, 4b). The same approach was used to build a clinical diagnostic model based on two independent descriptors (PTA

stage, P < 0.001; tinnitus fullness, P < 0.001). The AUCs of the clinical model in the training and validation cohorts were 0.915 (95% CI: 0.860–0.970) and 0.736 (95% CI: 0.617–0.855), respectively (Figures 4a, 4b).

Using multivariable logistic regression, four independent descriptors-Cochlea EH Grade, Vestibule\_EH, PTA Stage, and Tinnitus fullness-were identified for the combined DEMRI-clinical model (Table 3). The AUCs of the DEMRI-clinical model for diagnosing MD were 0.947 (95% CI: 0.903-0.990) in the training cohort and 0.796 (95% CI: 0.689-0.902) in the validation cohort (Figures 4a, 4b). De-Long's test was used to compare the correlated ROC curves. In the training set, the AUC of the DEMRI model was nearly equal to that of the clinical model. However, in the validation cohort, the DEMRI model had a significantly higher AUC (P = 0.012; 95% CI: 0.033–0.269). The DEMRI-clinical model also outperformed the clinical model in diagnosing MD (P =0.027). Although the DEMRI model had a slightly higher AUC than the DEMRI-clinical model, the difference was not statistically significant (P = 0.054) (Table 4).

The weights of the four independent risk factors used in the DEMRI model are illustrated in a nomogram (Figure 5a). The calibration curves of the DEMRI nomogram demonstrated good agreement in both the training and validation sets (Figures 5b, 5c).

Inter-observer agreement on the four magnetic resonance imaging features of the delayed post-gadolinium enhancement magnetic resonance imaging model

Inter-observer agreement for the four MRI features included in the DEMRI model was assessed using Kendall's W test. The features "Cochlea\_EH\_Grade," "Cochlea\_Apex\_EH\_

5,014 (0.607-46,332)

**Table 1.** A new weighted visual scoring criteria based on the Inner Ear Structural Assignment Method for inner ear 3D-FLAIR images

|                     |         | _      |      |                |                     |            |           |  |  |
|---------------------|---------|--------|------|----------------|---------------------|------------|-----------|--|--|
| Appearance          | Cochlea |        |      | Vestibule      | Semicircular canals |            |           |  |  |
|                     | Base    | Middle | Apex |                | Superior            | Horizontal | Posterior |  |  |
| Not visible#        | 0       | 0      | 0    | 0              | 0                   | 0          | 0         |  |  |
| Partially visible*  | 2       | 1      | _a   | 3 <sup>b</sup> | 1                   | 1          | 1         |  |  |
| Completely visible! | 3       | 2      | 1    | 6°             | 2                   | 2          | 2         |  |  |

Data represent scores awarded based on 3D-FLAIR images. \*Indicates the absence of a high-signal contrast medium. \*Refers to failure to show a high-signal image of the entire cochlear canal, a high-signal image limited to the tympanic or vestibular scala, interrupted high-signal images of the semicircular canals, or an incomplete high-signal image of the vestibule. \*Denotes that all labyrinth structures are completely visible. \*This option is not applicable, as the apex of the cochlea is very small; only a score of 0 or 1 is assigned. If visible, a score of 1 is given without distinguishing between partial and complete visibility. \*The hypointensity zone in the vestibule extends below the lower margin of the horizontal semicircular canal and is scored as 3. \*The hypointensity zone in the vestibule is located entirely above the plane of the horizontal semicircular canal and is scored as 6. 3D-FLAIR, three-dimensional fluid-attenuated inversion recovery.

| Variable                      | В       | Wald   | SE       | Р      | OR (95% CI)             |
|-------------------------------|---------|--------|----------|--------|-------------------------|
| (Intercept)                   | 30,073  | 0      | 2955.414 | 0.992  | 1.15E+13 (0-NA)         |
| Cochlea_EH_Grad               | 3.19    | 10,347 | 0.992    | 0.001* | 24,292 (5,058–297.868)  |
| Cochlea_Apex_EH_Score         | 3,698   | 4,298  | 1,784    | 0.038* | 40,384 (1,906–3014.737) |
| Vestibule_EH_Score            | 0.631   | 1,915  | 0.456    | 0.166  | 1,879 (0.852–5,211)     |
| Horizontal semicircular canal | -21,236 | 0      | 1477.708 | 0.989  | 0 (NA-1.91E+27)         |
| VA                            | 1,116   | 4,579  | 0.522    | 0.032* | 3,053 (1,196+9.632)     |
| Vestibule_EH                  | 3,729   | 6,663  | 1,445    | 0.010* | 41,631 (3.44-1172.845)  |

<sup>\*</sup>Statistically significant (P < 0.05). Data show multivariable regression results.

Table 2. Risk factors of DEMRI for MD in the training cohort

Cochlea\_EH\_Grad, Endolymphatic hydrops (EH) severity in the cochlea (0–3 grade); Cochlea\_Apex\_EH\_Score, EH in the cochlear apex (scored per Table 1); Vestibule\_EH\_Score, EH in the vestibule (scored per Table 1); Horizontal Semicircular Canal, Development (0 = absent, 1 = partial, 2 = complete); Vestibule\_EH, Presence/absence of vestibular EH (binary); VA, Vestibular aqueduct development (0 = absent, 1 = partial, 2 = complete); PE/MCPE, Perilymph-to-middle cerebellar peduncle signal intensity ratio; SE, standard error; OR, odds ratio; CI, confidence interval; DEMRI, delayed post-gadolinium enhancement magnetic resonance imaging; MD, Menière's disease.

2,332

1,056

0.127

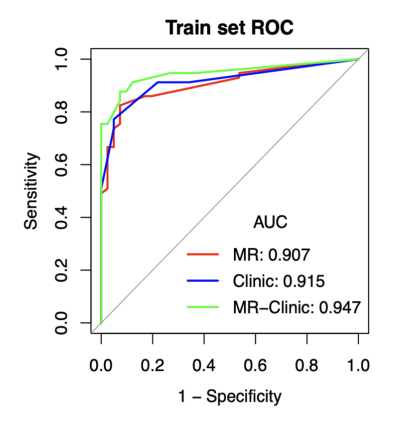
1,612

Score," "Vestibule\_EH," and "VA" all demonstrated very good consistency, with Kendall's coefficients of W = 0.954, 0.985, 0.967, and0.951, respectively. All associated P values were less than 0.001 (Supplementary Table 3).

# Discussion

In this study, we developed and validated three models to diagnose MD. The results showed that both the DEMRI model and the combined DEMRI-clinical model had better

clinical diagnostic performance than the clinical model alone (AUC: 0.736; sensitivity: 55.3%; specificity: 92.3%). The DEMRI model demonstrated excellent predictive performance in the validation set (AUC: 0.887; sensitivity: 78.9%; specificity: 88.5%). Although the AUC value of the combined DEMRI-clinical model was slightly lower than that of the DEMRI model, there was no significant difference in diagnostic performance. In the DEMRI model, the most substantial features



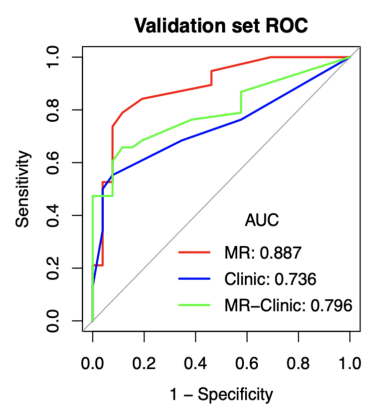


Figure 4. Receiver operating characteristic (ROC) curves. Performance of the three models in both the training and validation cohorts. AUC, area under the curve; MR, magnetic resonance.

**Table 3.** Risk factors of the DEMRI-clinical model for Menière's disease in the training cohort Variable Wald SE P OR (95% CI) (Intercept) -2.711 5.258 1.182 0.022 0.066 (0.005-0.531) Cochlea\_EH\_Grad 0.482 0.009\* 3.4989 (1.449-10.256) 1.252 6.755 Vestibule\_EH 1.377 2.996 0.796 0.083\* 3.964 (0.845-20.353) **PTA Stage** 1.581 5.911 0.65 0.015\* 4.861 (1.603-20.68) Tinnitus fullness -1.8215.988 0.744 0.014\* 0.162 (0.034-0.673)

Cochlea\_EH\_Grad: Cochlear endolymphatic hydrops severity grade (0-3)

Vestibule\_EH: Presence or absence of vestibular endolymphatic hydrops (binary)

PTA Stage: Hearing loss classification based on pure tone audiometry (0.5 kHz, 1 kHz, 2 kHz).

SE, standard error; OR, odds ratio; CI, confidence interval; DEMRI, delayed post-gadolinium enhancement magnetic resonance imaging

were "Cochlea\_EH\_Grad," "Cochlea\_Apex\_ EH Score," "VA," and "Vestibule EH."

MD is associated with a variety of comorbidities, such as migraine, anxiety, allergies, and immune disorders, but its pathogenesis remains unknown.27 EH, characterized by an increase in endolymphatic fluid within the membranous labyrinth of the inner ear, has been identified as the histopathological hallmark of MD. EH is thought to result from disrupted endolymph homeostasis caused by increased production, impaired absorption, or both.<sup>28</sup> In EH, excess endolymph volume leads to longitudinal flow from the cochlea to the endolymphatic sac (ES) to restore balance. Gibson<sup>29</sup> proposed that when the ES and endolymphatic duct (ED) are functional, they can remove excess endolymph. However, in patients with MD and dysfunctional ES and ED, endolymph may accumulate in the sinus of the ED, leading to substantial overflow. Various methods have been proposed to assess the endolymphatic space both qualitatively and quantitatively. 23,24,26 Studies have shown that the relationship between MD and EH is strong enough to consider EH a hallmark of MD and a sensitive target for diagnostic detection.12

In this study, significant differences were found in all MRI features related to EH between the MD and control groups (Supplementary Table 1). Amwwong these, three EH-related MRI features-"Cochlea\_EH\_Grad," "Cochlea\_Apex\_EH\_Score," and "Vestibule\_ EH"-were included in the DEMRI model. It appears that cochlea-related EH carries greater diagnostic weight in MD and that the presence or absence of hydrops in the cochlear apical turn is of particular diagnostic value.

It has been shown that cochlear hydrops follows a reliable pattern of hydropic pro-

| Table 4. Diagnostic performance of the three models in the training and validation cohorts |                    |             |             |       |             |          |  |  |  |
|--|--------------------|-------------|-------------|-------|-------------|----------|--|--|--|
| Model  | AUC (95% CI)       | Sensitivity | Specificity | PPV   | NPV         | Accuracy |  |  |  |
| DEMRI  |                    |             |             |       |             |          |  |  |  |
| Training cohort  | 0.907(0.848-0.966) | 0.825       | 0.927       | 0.940 | 0.792       | 0.867    |  |  |  |
| Validation cohort  | 0.887(0.802-0.971) | 0.789       | 0.885       | 0.909 | 0.742 0.828 | 0.828    |  |  |  |
| Clinical   |                    |             |             |       |             |          |  |  |  |
| Training cohort  | 0.915(0.860-0.970) | 0.772       | 0.951       | 0.957 | 0.75        | 0.847    |  |  |  |
| Validation cohort  | 0.736(0.617-0.855) | 0.553       | 0.923       | 0.913 | 0.585       | 0.703    |  |  |  |
| DEMRI-clinical   |                    |             |             |       |             |          |  |  |  |
| Training cohort  | 0.947(0.903-0.990) | 0.877       | 0.927       | 0.943 | 0.844       | 0.898    |  |  |  |
| Validation cohort  | 0.796(0.689-0.902) | 0.658       | 0.885       | 0.893 | 0.639       | 0.750    |  |  |  |

AUC, area under the receiver operating characteristic curve; CI, confidence interval; PPV, positive predictive value; NPV, negative predictive value. Model Features:

DEMRI model: Cochlea\_EH\_Grad, Cochlea\_Apex\_EH\_Score, VA, Vestibule\_EH

Clinical model: PTA Stage, Tinnitus fullness

DEMRI-clinical model: Cochlea\_EH\_Grad, Vestibule\_EH, PTA Stage, Tinnitus fullness.

<sup>\*</sup>Statistically significant (P < 0.05).Multivariable regression results show:

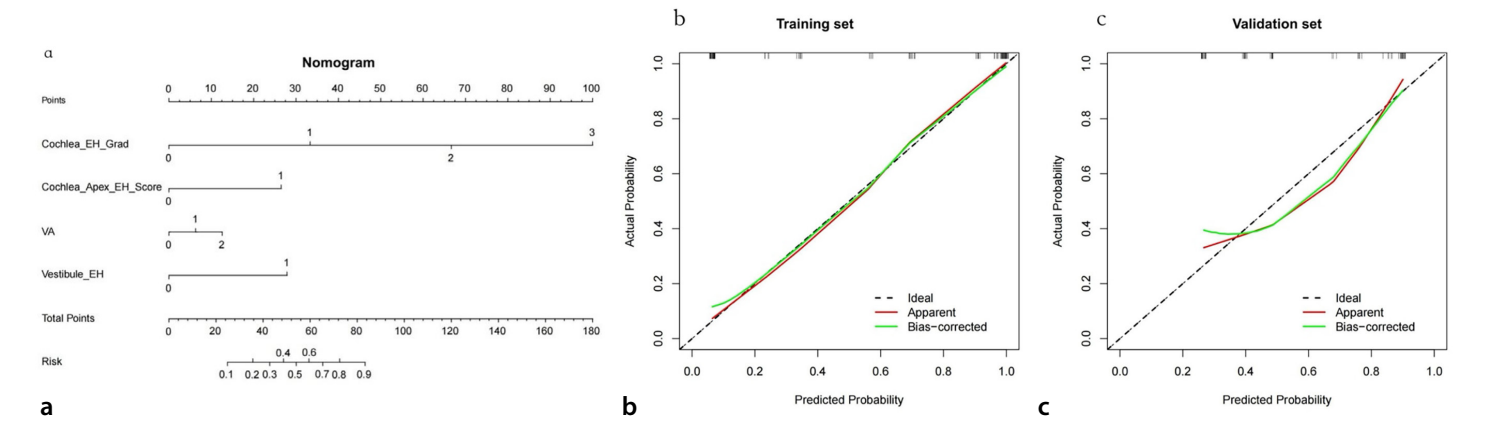


Figure 5. The DEMRI nomogram constructed in the training cohort using Cochlea\_EH\_Grad, Cochlea\_Apex\_EH\_Score, VA, and Vestibule\_EH (a). Calibration curves of the nomogram in the (b) training and (c) validation cohorts. DEMRI, delayed post-

gression over time, typically originating in the apex and proceeding toward the base, tonotopically resembling the progression of hearing loss. 12,30,31 A hydrodynamic pressure shunt in the pars superior stimulates the utricle and the saccule of the vestibule, resulting in "Vestibule\_EH".28,29 This longitudinal hydrops process may explain why the presence or absence of EH in the apical turn of the cochlea is diagnostically substantial for MD. Additionally, experimental studies have suggested that cytochemical and ultrastructural disruption of the hair cells, afferent neurons, and fibrocytes of the lateral cochlear wall are involved in the pathogenesis of EH and occur prior to its development. 10,32,33 These findings support the conclusion that "Cochlea\_EH\_ Grad" and "Vestibule\_EH" are important risk factors for diagnosing MD. It is important to consider both the grade of EH in the cochlea and the presence or absence of EH in the vestibule. The more severe the cochlear EH, the higher the likelihood of diagnosing MD when accompanied by vestibular EH, regardless of the severity of the vestibular component.

However, EH is not pathognomonic for MD, as it has also been observed in vestibular migraine (VM), isolated SNHL, and even in healthy individuals. This limits its diagnostic specificity for MD.5,34 VM is a leading cause of recurrent vertigo and is often misdiagnosed as MD despite being 5-10 times more prevalent.35 The clinical overlap between MD and VM presents substantial diagnostic challenges. Emerging evidence suggests that differences in EH patterns may help distinguish the two conditions: MD typically presents with both cochlear and vestibular EH (as seen on Gd-enhanced MRI), whereas EH in VM is rare and usually limited to the cochlea.35-37 Thus, inner ear imaging (e.g., Gd-DEMRI) may assist in differential diagnosis. Isolated SNHL may represent a prodromal phase of MD and warrants further investigation.

Furthermore, this study identified a relatively novel finding: the VA appears to be a substantial risk factor in diagnosing MD. A study by Steve Connor et al.15 demonstrated that all VA descriptors showed excellent reliability for MD diagnosis and that incomplete VA visualization adds diagnostic value. Mainnemarre et al.16 further suggested that evaluating the VA on temporal bone computed tomography (CT) could predict the presence of EH on MRI with a high positive predictive value. Attyé et al.38 proposed that discontinuous VA may correlate with MD. A non-visible or partially visible VA may result from bony abnormalities or central fibrosis, leading to endolymphatic stenosis. Although VA performance was included in our model, there was no statistically significant difference in VA between the MD and control groups (Supplementary File). This may be due to the low detection rate of VA on MRI, highlighting the need for clearer imaging techniques or combining MRI with other modalities, such as CT, for more comprehensive evaluation.

Following large-scale validation, our diagnostic model could be incorporated into clinical practice to generate structured radiology reports with probability scores. These reports could support the following: (1) risk stratification, (2) identification of high-risk patients needing specialist referral, and (3) long-term post-treatment management.

# Limitations

**Limited sample size:** Although this is a multicenter study, the sample size (85 patients, 162 ears) is relatively small, which may limit the generalizability of the findings. Future studies with larger cohorts are needed

to validate these results.

Retrospective design: The retrospective nature of the study introduces potential biases in patient selection and data collection. Additionally, some asymptomatic patients with early MD may have been misclassified into the control group. Future research should include normal participants and other differential diagnoses (e.g., VM, benign positional vertigo) for more robust comparisons.

Lack of external validation: Although internal validation was performed, external validation using an independent dataset would further strengthen the reliability of the model.

Imaging feature selection: This study primarily relied on conventional MRI features. Further exploration of advanced imaging biomarkers may improve diagnostic accuracy.

In conclusion, we developed and validated a new DEMRI model for diagnosing MD, which demonstrated higher diagnostic value than clinical inquiry information alone. A combination of a high degree of cochlear EH, invisible cochlear apical turn, vestibular hydrops, and incomplete VA visualization suggests a high risk of MD. Therefore, we recommend DEMRI when MD is suspected due to its substantial diagnostic potential. Further studies are needed to explore the broader applicability of our model and support its clinical implementation.

### **Footnotes**

# Conflict of interest disclosure

The authors declared no conflicts of interest.

# **Funding**

This work was supported by the National Natural Science Foundation of China (Grant ID: 82202089).

# References

- Rizk HG, Mehta NK, Qureshi U, et al. Pathogenesis and etiology of Meniere disease: a scoping review of a century of evidence. JAMA Otolaryngol Head Neck Surg. 2022;148(4):360-368. [Crossref]
- Minor LB, Schessel DA, Carey JP. Ménière's disease. Curr Opin Neurol. 2004;17(1):9-16.
   [Crossref]
- 3. Sajjadi H, Paparella MM. Meniere's disease. *Lancet*. 2008;372(9636):406-414. [Crossref]
- Committee on Hearing and Equilibrium guidelines for the diagnosis and evaluation of therapy in Menière's disease. American Academy of Otolaryngology-Head and Neck Foundation, Inc. Otolaryngol Head Neck Surg. 1995;113(3):181-185. [Crossref]
- Hoskin JL. Meniere's disease: new guidelines, subtypes, imaging, and more. Curr Opin Neurol. 2022;35(1):90-97. [Crossref]
- Lopez-Escamez JA, Carey J, Chung WH, et al. Diagnostic criteria for Meniere's disease. J Vestib Res. 2015; 25(1):1-7. [Crossref]
- Hallpike CS, Cairns H. Observations on the pathology of Ménière's syndrome: (section of otology). Proc R Soc Med. 1938;31(11):1317-36.
   [Crossref]
- Gurkov R, Pyyko I, Zou J, Kentala E. What is Meniere's disease? A contemporary reevaluation of endolymphatic hydrops. J Neurol. 2016;263(Suppl 1):71-81. [Crossref]
- Nakashima T, Naganawa S, Sugiura M, et al. Visualization of endolymphatic hydrops in patients with Meniere's disease. *Laryngoscope*. 2007;117(3):415-420. [Crossref]
- Fiorino F, Pizzini FB, Beltramello A, Barbieri F. Progression of endolymphatic hydrops in Ménière's disease as evaluated by magnetic resonance imaging. Otol Neurotol. 2011;32:1152-1157. [Crossref]
- Connor SEJ, Pai I. Endolymphatic hydrops magnetic resonance imaging in Meniere's disease. Clin Radiol. 2021;76(1):76. [Crossref]
- Gluth MB. On the relationship between Meniere's Disease and endolymphatic hydrops. Otol Neurotol. 2020;41(2):242-249.
   [Crossref]
- Li J, Jin X, Kong X, et al. Correlation of endolymphatic hydrops and perilymphatic enhancement with the clinical features of Meniere's disease. Eur Radiol. 2024;34(9):6036-6046. [Crossref]
- van Steekelenburg JM, van Weijnen A, de Pont LMH, et al. Value of endolymphatic hydrops and perilymph signal intensity in suspected Meniere Disease. AJNR Am J Neuroradiol. 2020;41(3):529-534. [Crossref]

- Connor S, Pai I, Touska P, McElroy S, Ourselin S, Hajnal JV. Assessing the optimal MRI descriptors to diagnose Meniere's disease and the added value of analysing the vestibular aqueduct. Eur Radiol. 2024;34(9):6060-6071.
   [Crossref]
- Mainnemarre J, Hautefort C, Toupet M, et al. The vestibular aqueduct ossification on temporal bone CT: an old sign revisited to rule out the presence of endolymphatic hydrops in Meniere's disease patients. Eur Radiol. 2020;30(11):6331-6338. [Crossref]
- Connor S, Grzeda MT, Jamshidi B, Ourselin S, Hajnal JV, Pai I. Delayed post gadolinium MRI descriptors for Meniere's disease: a systematic review and meta-analysis. Eur Radiol. 2023;33(10):7113-7135. [Crossref]
- Chen W, Yu S, Xiao H, et al. A novel radiomics nomogram based on T2-sampling perfection with application-optimized contrasts using different flip-angle evolutions (SPACE) images for predicting cochlear and vestibular endolymphatic hydrops in Meniere's disease patients. *Eur Radiol.* 2024;34(9):6082-6091. [Crossref]
- Kobayashi M, Yoshida T, Fukunaga Y, Hara D, Naganawa S, Sone M. Perilymphatic enhancement and endolymphatic hydrops: MRI findings and clinical associations. Laryngoscope Investig Otolaryngol. 2024;9(5):e1312. [Crossref]
- van den Burg EL, van Hoof M, Postma AA, et al. An exploratory study to detect Meniere's disease in conventional MRI scans using radiomics. Front Neurol. 2016;7:190. [Crossref]
- Eliezer M, Poillon G, Gillibert A, et al.
   Comparison of enhancement of the vestibular perilymph between gadoterate meglumine and gadobutrol at 3-Tesla in Meniere's disease.
   Diagn Interv Imaging. 2018;99(5):271-277.
   [Crossref]
- Xie J, Zhang W, Zhu J, Hui L, Li S, Zhang B. Comparison of inner ear MRI enhancement in patients with Meniere's disease after intravenous injection of gadobutrol, gadoterate meglumine, or gadodiamide. Eur J Radiol. 2021;139:109682. [Crossref]
- Gurkov R, Flatz W, Louza J, Strupp M, Krause E. In vivo visualization of endolyphatic hydrops in patients with Meniere's disease: correlation with audiovestibular function. *Eur Arch Otorhinolaryngol*. 2011;268(12):1743-1748.
   [Crossref]
- Bernaerts A, Vanspauwen R, Blaivie C, et al. The value of four stage vestibular hydrops grading and asymmetric perilymphatic enhancement in the diagnosis of Meniere's disease on MRI. Neuroradiology. 2019; 61(4):421-429. [Crossref]
- 25. Fang ZM, Chen X, Gu X, et al. A new magnetic resonance imaging scoring system for perilymphatic space appearance after

- intratympanic gadolinium injection, and its clinical application. *J Laryngol Otol.* 2012;126(5):454-459. [Crossref]
- Xiao H, Guo X, Cai H, et al. Magnetic resonance imaging of endolymphatic hydrops in Meniere's disease: a comparison of the diagnostic value of multiple scoring methods. Front Neurol. 2022;13:967323. [Crossref]
- Lopez-Escamez JA, Liu Y. Epidemiology and genetics of Meniere's disease. Curr Opin Neurol. 2024;37(1):88-94. [Crossref]
- 28. Mohseni-Dargah M, Falahati Z, Pastras C, et al. Meniere's disease: pathogenesis, treatments, and emerging approaches for an idiopathic bioenvironmental disorder. *Environ Res*. 2023;238(Pt 1):116972. [Crossref]
- Gibson WP. Hypothetical mechanism for vertigo in Meniere's disease. Otolaryngol Clin North Am. 2010;43(5):1019-1027. [Crossref]
- Wu Q, Dai C, Zhao M, Sha Y. The correlation between symptoms of definite Meniere's disease and endolymphatic hydrops visualized by magnetic resonance imaging. Laryngoscope. 2016;126(4):974-979. [Crossref]
- Li J, Wang L, Hu N, et al. Longitudinal variation of endolymphatic hydrops in patients with Meniere's disease. *Ann Transl Med*. 2023;11(2):44. [Crossref]
- 32. Nadol JB, Adams JC, Kim JR. Degenerative changes in the organ of corti and lateral cochlear wall in experimental endolymphatic hydrops and human Menière's disease. *Acta Otolaryngol Suppl.* 1995; 519:47-59. [Crossref]
- Ichimiya I, Adams JC, Kimura RS. Changes in immunostaining of cochleas with experimentally induced endolymphatic hydrops. Ann Otol Rhinol Laryngol. 1994;103(6):457-468. [Crossref]
- Lingam RK, Connor SEJ, Casselman JW, Beale T. MRI in otology: applications in cholesteatoma and Meniere's disease. Clin Radiol. 2018;73(1):35-44. [Crossref]
- Chen JY, Guo ZQ, Wang J, et al. Vestibular migraine or Meniere's disease: a diagnostic dilemma. J Neurol. 2023;270(4):1955-1968.
   [Crossref]
- Nakada T, Yoshida T, Suga K, et al. Endolymphatic space size in patients with vestibular migraine and Meniere's disease. J Neurol. 2014;261(11):2079-2084. [Crossref]
- 37. Sun W, Guo P, Ren T, Wang W. Magnetic resonance imaging of intratympanic gadolinium helps differentiate vestibular migraine from Meniere disease. *Laryngoscope*. 2017;127(10):2382-2388. [Crossref]
- Attyé A, Barma M, Schmerber S, Dumas G, Eliezer M, Krainik A. The vestibular aqueduct sign: magnetic resonance imaging can detect abnormalities in both ears of patients with unilateral Meniere's disease. *J Neuroradiol*. 2020;47(2):174-179. [Crossref]

| Supplementary Table 1. Compariontrol group and MD group | Supplementary Table 1. Comparison of clinical variables and MRI features between control group and MD group |                            |               |  |  |  |  |  |
|---|---|----------------------------|---------------|--|--|--|--|--|
|   | Control ears<br>(n = 67)  | Menière's ears<br>(n = 95) | P value       |  |  |  |  |  |
| PTA stage   |   |                            |               |  |  |  |  |  |
| 1   | 52 (77.6%)  | 27 (28.4%)                 | <0.001        |  |  |  |  |  |
| 2   | 13 (19.4%)  | 21 (22.1%)                 |               |  |  |  |  |  |
| 3   | 2 (3.0%)  | 31 (32.6%)                 |               |  |  |  |  |  |
| 4   | 0 (0%)  | 16 (16.8%)                 |               |  |  |  |  |  |
| Vertigo   |   |                            |               |  |  |  |  |  |
|   | 49 (73.1%)  | 92 (96.8%)                 | <0.001        |  |  |  |  |  |
| Tinnitus fullness                                       |   |                            |               |  |  |  |  |  |
|   | 17 (25.4%)  | 71 (74.7%)                 | <0.001        |  |  |  |  |  |
| Age   |   |                            |               |  |  |  |  |  |
| Mean (SD)   | 49.9 (13.1)   | 55.5 (13.6)                | 0.009         |  |  |  |  |  |
| Gender  |   |                            |               |  |  |  |  |  |
| Male/female   | 33/34   | 43/52                      | 0.733         |  |  |  |  |  |
| BMI   |   |                            |               |  |  |  |  |  |
| Mean (SD)   | 23.0 (2.40)   | 22.7 (2.70)                | 0.426         |  |  |  |  |  |
| Cochlea_Base_EH_Grad                                    |   |                            |               |  |  |  |  |  |
| 0   | 63 (94.0%)  | 41 (43.2%)                 | <0.001        |  |  |  |  |  |
| 1   | 1 (1.5%)  | 22 (23.2%)                 |               |  |  |  |  |  |
| 2   | 3 (4.5%)  | 17 (17.9%)                 |               |  |  |  |  |  |
| 3   | 0 (0%)  | 15 (15.8%)                 |               |  |  |  |  |  |
| Cochlea_Middle_EH_Grad                                  | 0 (0 /0)  | 15 (15.670)                |               |  |  |  |  |  |
| 0   | 63 (94.0%)  | 40 (42.1%)                 | <0.001        |  |  |  |  |  |
| 1   | 2 (3.0%)  | 14 (14.7%)                 | 101001        |  |  |  |  |  |
| 2   | 2 (3.0%)  | 16 (16.8%)                 |               |  |  |  |  |  |
| 3   | 0 (0%)  | 25 (26.3%)                 |               |  |  |  |  |  |
| Cochlea_Apex_EH_Grad                                    | 0 (070)   | 25 (20.570)                |               |  |  |  |  |  |
| 0   | 62 (92.5%)  | 35 (36.8%)                 | <0.001        |  |  |  |  |  |
| 1   | 2 (3.0%)  | 16 (16.8%)                 | <b>\0.001</b> |  |  |  |  |  |
| 2   | 3 (4.5%)  | 19 (20.0%)                 |               |  |  |  |  |  |
| 3   | 0 (0%)  | 25 (26.3%)                 |               |  |  |  |  |  |
| Cochlea_EH_Grad   | 0 (070)   | 25 (20.570)                |               |  |  |  |  |  |
| 0   | 61 (91.0%)  | 25 (26.3%)                 | <0.001        |  |  |  |  |  |
| 1   | 3 (4.5%)  | 24 (25.3%)                 | \0.00T        |  |  |  |  |  |
| 2   | 3 (4.5%)  | 21 (22.1%)                 |               |  |  |  |  |  |
| 3   | 0 (0%)  | 25 (26.3%)                 |               |  |  |  |  |  |
| Cochlea_Base_EH_Score                                   | 0 (070)   | 23 (20.3%)                 |               |  |  |  |  |  |
| O Cocniea_Base_En_Score                                 | 0 (0%)  | 2 (2.1%)                   | <0.001        |  |  |  |  |  |
| 2   | 4 (6.0%)  | 53 (55.8%)                 | \0.001        |  |  |  |  |  |
| 3   | 4 (6.0%)  | 40 (42.1%)                 |               |  |  |  |  |  |
|   | 05 (54.070)   | 40 (42.170)                |               |  |  |  |  |  |
| Cochlea_Middle_EH_Score                                 | 0 (0%)  | 12 (12 60/)                | <0.001        |  |  |  |  |  |
| 0   | 0 (0%)  | 12 (12.6%)                 | <0.001        |  |  |  |  |  |
| 1   | 4 (6.0%)  | 45 (47.4%)                 |               |  |  |  |  |  |
| Cochles Apply EU Score                                  | 63 (94.0%)  | 38 (40.0%)                 |               |  |  |  |  |  |
| Cochlea_Apex_EH_Score                                   | 4 (6 00%)   | 24 (25 00/)                | 40.00¢        |  |  |  |  |  |
| 0   | 4 (6.0%)  | 34 (35.8%)                 | <0.001        |  |  |  |  |  |
| 1   | 63 (94.0%)  | 61 (64.2%)                 |               |  |  |  |  |  |
| Cochlea_EH_Score  |   |                            |               |  |  |  |  |  |

| Supplementary Table 1. Continued |                       |                            |         |
|----------------------------------|-----------------------|----------------------------|---------|
|                                  | Control ears (n = 67) | Menière's ears<br>(n = 95) | P value |
| 0                                | 0 (0%)                | 1 (1.1%)                   | <0.001  |
| 2                                | 0 (0%)                | 10 (10.5%)                 |         |
| 3                                | 1 (1.5%)              | 12 (12.6%)                 |         |
| 4                                | 4 (6.0%)              | 31 (32.6%)                 |         |
| 5                                | 1 (1.5%)              | 12 (12.6%)                 |         |
| 6                                | 61 (91.0%)            | 29 (30.5%)                 |         |
| Vestibule_EH_Score               |                       |                            |         |
| 0                                | 0 (0%)                | 15 (15.8%)                 | <0.001  |
| 3                                | 13 (19.4%)            | 45 (47.4%)                 |         |
| 4                                | 54 (80.6%)            | 35 (36.8%)                 |         |
| Vestibule_EH_Grade               |                       |                            |         |
| 0                                | 57 (85.1%)            | 30 (31.6%)                 | <0.001  |
| 1                                | 8 (11.9%)             | 19 (20.0%)                 |         |
| 2                                | 2 (3.0%)              | 17 (17.9%)                 |         |
| 3                                | 0 (0%)                | 29 (30.5%)                 |         |
| Semicircular canal superior      |                       |                            |         |
| Non-visualized                   | 0 (0%)                | 5 (5.3%)                   | 0.035   |
| Incompletely visualized          | 0 (0%)                | 4 (4.2%)                   |         |
| Completely visualized            | 67 (100%)             | 86 (90.5%)                 |         |
| Semicircular canal horizontal    |                       |                            |         |
| Non-visualized                   | 0 (0%)                | 9 (9.5%)                   | <0.001  |
| Incompletely visualized          | 0 (0%)                | 18 (18.9%)                 |         |
| Completely visualized            | 67 (100%)             | 68 (71.6%)                 |         |
| Semicircular canal posterior     |                       |                            |         |
| Non-visualized                   | 0 (0%)                | 5 (5.3%)                   | 0.023   |
| Incompletely visualized          | 0 (0%)                | 5 (5.3%)                   |         |
| Completely visualized            | 67 (100%)             | 85 (89.5%)                 |         |
| VA                               |                       |                            |         |
| Non-visualized                   | 23 (34.3%)            | 41 (43.2%)                 | 0.318   |
| Incompletely visualized          | 20 (29.9%)            | 30 (31.6%)                 |         |
| Completely visualized            | 24 (35.8%)            | 24 (25.3%)                 |         |
| Cochlea_EH                       |                       |                            |         |
| EH-positive                      | 60 (89.6%)            | 25 (26.3%)                 | <0.001  |
| Vestibule_EH                     |                       |                            |         |
| EH-positive                      | 57 (85.1%)            | 30 (31.6%)                 | <0.001  |
| PLE/MCPE                         |                       |                            |         |
| Mean (SD)                        | 1.15 (0.291)          | 1.33 (0.368)               | <0.001  |
| Group                            |                       |                            |         |
| Training set                     | 41 (61.2%)            | 57 (60.0%)                 | 1       |
| Validation set                   | 26 (38.8%)            | 38 (40.0%)                 |         |
|                                  |                       |                            |         |

 $Coch lear and vestibular endolymphatic \ hydrops \ were \ evaluated \ according \ to \ Gurkov \ and \ Bernaerts' \ visual \ 4-grade \ method.$ 

Cochlear and vestibular endolymphatic hydrops scorewere evaluated according to a new weighted visual scoring system (Table 1) based on Inner Ear Structural Assignment Method.

PLE/MCPE: Measurements of signal intensity were performed by drawing an oval region of interest along the edge of the cochlear basal turn and a circular region of interest at the left middle cerebellar peduncle to calculate the signal intensity ratio.

PTA, pure tone audiometry; SD, standard deviation; BMI, body mass index; VA, vestibular aqueduct; PLE, perilymphatic enhancement; MCPE, middle cerebellar peduncle.

|                         |                          | ) ( le le                 |         |
|-------------------------|--------------------------|---------------------------|---------|
|                         | Training set<br>(n = 98) | Validation set $(n = 64)$ | P value |
| Label                   |                          |                           |         |
| Control ears            | 41 (41.8%)               | 26 (40.6%)                | 1       |
| Menière's ears          | 57 (58.2%)               | 38 (59.4%)                |         |
| PTA stage               |                          |                           |         |
| 1                       | 47 (48.0%)               | 32 (50.0%)                | 0.972   |
| 2                       | 20 (20.4%)               | 14 (21.9%)                |         |
| 3                       | 21 (21.4%)               | 12 (18.8%)                |         |
| 4                       | 10 (10.2%)               | 6 (9.4%)                  |         |
| Vertigo                 |                          |                           |         |
|                         | 90 (91.8%)               | 51 (79.7%)                | 0.044   |
| Tinnitus fullness       |                          |                           |         |
|                         | 41 (41.8%)               | 33 (51.6%)                | 0.292   |
| Age                     |                          |                           |         |
| Mean (SD)               | 53.4 (13.0)              | 53.0 (14.6)               | 0.852   |
| Gender                  |                          |                           |         |
| Male/female             | 43/55                    | 33/31                     | 0.425   |
| BMI                     |                          |                           |         |
| Mean (SD)               | 23.0 (2.59)              | 22.4 (2.54)               | 0.165   |
| Cochlea_Base_EH_Grad    |                          | (,                        |         |
| 0                       | 61 (62.2%)               | 43 (67.2%)                | 0.757   |
| 1                       | 14 (14.3%)               | 9 (14.1%)                 | 0.757   |
| 2                       | 12 (12.2%)               | 8 (12.5%)                 |         |
| 3                       | 11 (11.2%)               | 4 (6.3%)                  |         |
| Cochlea_Middle_EHGrad   | 11 (11.270)              | 4 (0.5 %)                 |         |
| 0                       | 60 (61.2%)               | 43 (67.2%)                | 0.75    |
| 1                       | 9 (9.2%)                 | 7 (10.9%)                 | 0.75    |
| 2                       |                          |                           |         |
|                         | 12 (12.2%)               | 6 (9.4%)                  |         |
| Saddan Array Ell Cond   | 17 (17.3%)               | 8 (12.5%)                 |         |
| Cochlea_Apex_EH_Grad    | FC (F7 10()              | 41 (64 10/)               | 0.653   |
| 0                       | 56 (57.1%)               | 41 (64.1%)                | 0.653   |
| 1                       | 10 (10.2%)               | 8 (12.5%)                 |         |
| 2                       | 15 (15.3%)               | 7 (10.9%)                 |         |
| 3                       | 17 (17.3%)               | 8 (12.5%)                 |         |
| Cochlea_EH_Grad         | /                        | 25 (5: 5: )               | 0.21    |
| 0                       | 51 (52.0%)               | 35 (54.7%)                | 0.84    |
| 1                       | 15 (15.3%)               | 12 (18.8%)                |         |
| 2                       | 16 (16.3%)               | 8 (12.5%)                 |         |
| 3                       | 16 (16.3%)               | 9 (14.1%)                 |         |
| Cochlea_Base_EH_Score   |                          |                           |         |
| 0                       | 2 (2.0%)                 | 0 (0%)                    | 0.498   |
| 2                       | 35 (35.7%)               | 22 (34.4%)                |         |
| 3                       | 61 (62.2%)               | 42 (65.6%)                |         |
| Cochlea_Middle_EH_Score |                          |                           |         |
| 0                       | 10 (10.2%)               | 2 (3.1%)                  | 0.235   |
| 1                       | 28 (28.6%)               | 21 (32.8%)                |         |
| 2                       | 60 (61.2%)               | 41 (64.1%)                |         |
| Cochlea_Apex_EH_Score   |                          |                           |         |

| Supplementary Table 2. Continued   |                          |                            |         |
|--|--------------------------|----------------------------|---------|
|  | Training set<br>(n = 98) | Validation set<br>(n = 64) | P value |
| 0  | 26 (26.5%)               | 12 (18.8%)                 | 0.341   |
| 1  | 72 (73.5%)               | 52 (81.3%)                 |         |
| Cochlea_EH_Score   |                          |                            |         |
| 0  | 1 (1.0%)                 | 0 (0%)                     | 0.427   |
| 2  | 8 (8.2%)                 | 2 (3.1%)                   |         |
| 3  | 8 (8.2%)                 | 5 (7.8%)                   |         |
| 4  | 21 (21.4%)               | 14 (21.9%)                 |         |
| 5  | 5 (5.1%)                 | 8 (12.5%)                  |         |
| 6  | 55 (56.1%)               | 35 (54.7%)                 |         |
| Vestibule_EH_Score   |                          |                            |         |
| 0  | 11 (11.2%)               | 4 (6.3%)                   | 0.562   |
| 3  | 34 (34.7%)               | 24 (37.5%)                 |         |
| 6  | 53 (54.1%)               | 36 (56.3%)                 |         |
| Vestibule_EH_Grade   |                          |                            |         |
| 0  | 52 (53.1%)               | 35 (54.7%)                 | 0.617   |
| 1  | 14 (14.3%)               | 13 (20.3%)                 |         |
| 2  | 12 (12.2%)               | 7 (10.9%)                  |         |
| 3  | 20 (20.4%)               | 9 (14.1%)                  |         |
| Semicircular canal superior  |                          |                            |         |
| Non-visualized   | 4 (4.1%)                 | 1 (1.6%)                   | 0.61    |
| Incompletely visualized  | 2 (2.0%)                 | 2 (3.1%)                   |         |
| Completely visualized  | 92 (93.9%)               | 61 (95.3%)                 |         |
| Semicircular canal horizontal  |                          |                            |         |
| Non-visualized   | 6 (6.1%)                 | 3 (4.7%)                   | 0.772   |
| Incompletely visualized  | 12 (12.2%)               | 6 (9.4%)                   |         |
| Completely visualized  | 80 (81.6%)               | 55 (85.9%)                 |         |
| Semicircular canal posterior   |                          |                            |         |
| Non-visualized   | 3 (3.1%)                 | 2 (3.1%)                   | 0.999   |
| Incompletely visualized  | 3 (3.1%)                 | 2 (3.1%)                   |         |
| Completely visualized  | 92 (93.9%)               | 60 (93.8%)                 |         |
| VA   |                          |                            |         |
| Non-visualized   | 37 (37.8%)               | 27 (42.2%)                 | 0.766   |
| Incompletely visualized  | 30 (30.6%)               | 20 (31.3%)                 |         |
| Completely visualized  | 31 (31.6%)               | 17 (26.6%)                 |         |
| Cochlea_EH   |                          |                            |         |
| EH-positive  | 51 (52.0%)               | 34 (53.1%)                 | 1       |
| Vestibule_EH   |                          |                            |         |
| EH-positive  | 52 (53.1%)               | 35 (54.7%)                 | 0.967   |
| PE/MCPE  |                          |                            |         |
| Mean (SD)  | 1.21 (0.318)             | 1.32 (0.386)               | 0.065   |
| PTA, pure tone audiometry; SD, standard deviation; B perilymphatic enhancement; MCPE, middle cerebella | •                        | A, vestibular aqueduct;    | PLE,    |

| Supplementary Table 3. Inter-observer reliability Kendall'W values for the four DEMRI model features |           |                         |          |             |                    |     |              |    |      |    |    |
|--|-----------|-------------------------|----------|-------------|--------------------|-----|--------------|----|------|----|----|
| Grade/score  | Coch      | Cochlea_EH_Grade        |          | Cochlea_Ape | Cochlea_Apex_Score |     | Vestibule_EH |    | VA   |    |    |
|  | 0         | 1                       | 2        | 3           | 0                  | 1   | Yes          | No | 0    | 1  | 2  |
| Observer1  | 84        | 29                      | 26       | 23          | 38                 | 124 | 75           | 87 | 66   | 48 | 48 |
| Observer2  | 79        | 38                      | 32       | 13          | 40                 | 122 | 71           | 91 | 73   | 45 | 44 |
| Observer3  | 81        | 32                      | 25       | 24          | 38                 | 124 | 75           | 87 | 66   | 57 | 39 |
| Kendall's W  | 0.954     | 0.954 0.985 0.967 0.951 |          |             |                    |     |              |    | 1    |    |    |
| P  | <0.00     | )1                      |          |             | <0.001             |     | < 0.001      |    | <0.0 | 01 |    |
| VA, vestibular aqueduct; DEMRI, delayed post-  | gadoliniu | n enhan                 | cement m | agnetic re  | sonance imaging.   |     |              |    |      |    |    |